American Society of Hematology
2021 L Street NW, Suite 900,
Washington, DC 20036
Phone: 202-776-0544 | Fax 202-776-0545
editorial@hematology.org

First-hit SETBP1 mutations cause a myeloproliferative disorder with bone marrow fibrosis

Tracking no: BLD-2023-021349R2

Ilaria Crespiatico (University of Milano Bicocca, Italy) Mattia Zaghi (IRCCS San Raffaele Scientific Institute, Italy) Cristina Mastini (University of Milano-Bicocca, Italy) Deborah D'Aliberti (University of Milano-Bicocca, Italy) Mario Mauri (University of Milano Bicocca, Italy) Carl Mercado (University of Milano-Bicocca, Italy) Diletta Fontana (University of Milano Bicocca, Italy) Silvia Spinelli (University of Milano-Bicocca, Italy) Valentina Crippa (University of Milano-Bicocca, Italy) Elena Inzoli (San Gerardo Hospital, Italy) Beatrice Manghisi (San Gerardo Hospital, Italy) Ivan Civettini (University of Milano-Bicocca, Italy) Daniele Ramazzotti (University of Milano - Bicocca, Italy) Valentina Sangiorgio (San Gerardo Hospital, Italy) michele gengotti (University of Milano - Bicocca, Italy) Virginia Brambilla (University Milan Bicocca, Italy) Andrea Aroldi (Hematology Division and Bone Marrow Unit, San Gerardo Hospital; Monza, Italy, Italy) federica banfi (IRCCS San Raffaele Scientific Institute, Italy) Cristiana Barone (University of Milano Bicocca, Italy) roberto orsenigo (Vall d'Hebron Research Institute (VHIR), Vall d'Hebron Hospital Barcelona-UAB, Spain) LUDOVICA RIERA (UNIVERSITY OF TORINO, Italy) MARA RIMINUCCI (SAPIENZA UNIVERSITY OF ROME, Italy) Alessandro Corsi (SAPIENZA UNIVERSITY OF ROME, Italy) Massimo Breccia (Hematology-Sapienza University, Italy) Alessandro Morotti (University of Turin, Italy) Daniela Cilloni (University of Turin, Italy) Aldo Roccaro (ASST Spedali Civili di Brescia, Italy) Antonio Sacco (ASST Spedali Civili di Brescia, Italy) Fabio Stagno (Hematology Section, Policlinico Hospital, Building H AOU Policlinico - G. Bertino, Italy) Marta Serafini (Tettamanti Center, Fondazione IRCCS San Gerardo dei Tintori, Italy) Federica Mottadelli (Tettamanti Center, Fondazione IRCCS San Gerardo dei Tintori, Italy) Giovanni Cazzaniga (Centro Tettamanti, IRCCS San Gerardo dei Tintori, Monza, Italy, Italy) Fabio Pagni (University Milan Bicocca, Italy) Roberto Chiarle (Department of Pathology, Children's Hospital and Harvard Medical School, Boston, MA, USA, United States) Emanuele Azzoni (University of Milano Bicocca, Italy) Alessandro Sessa (IRCCS San Raffaele Scientific Institute, Italy) Carlo Gambacorti-Passerini (3Hematology Division and Bone Marrow Unit, San Gerardo Hospital, Monza, Italy, Italy) Elena Elli (Hematology Division and Bone Marrow Unit, Ospedale San Gerardo, ASST Monza e Brianza, Italy) Luca Mologni (University of Milano-Bicocca, Italy) Rocco Piazza (Hematology Division and Bone Marrow Unit, San Gerardo Hospital; Monza, Italy, Italy)

Abstract:
SETBP1 mutations are found in various clonal myeloid disorders. However, it is unclear whether they can initiate leukemia, as SETBP1 mutations typically appear as later events during oncogenesis. To answer this question, we generated a mouse model expressing mutated SETBP1 in hematopoietic tissue: this model showed profound alterations in the differentiation program of hematopoietic progenitors and developed a myeloid neoplasm with megakaryocytic dysplasia, splenomegaly, and bone marrow fibrosis, prompting us to investigate SETBP1 mutations in a cohort of 36 triple-negative primary myelofibrosis (TN-PMF) cases. We identified two distinct subgroups, one carrying SETBP1 mutations and the other completely devoid of somatic variants. Clinically, a striking difference in disease aggressiveness was noted, with SETBP1-mutated patients showing a much worse clinical course. As opposite to myelodysplastic/myeloproliferative neoplasms, where SETBP1 mutations are mostly found as a late clonal event, single-cell clonal hierarchy reconstruction in three TN-PMF patients from our cohort revealed SETBP1 to be a very early event, suggesting that the phenotype of the different SETBP1+ disorders may be shaped by the opposite hierarchy of the same clonal SETBP1 variants.-

Conflict of interest: No COI declared

COI notes:

Preprint server: No;

Author contributions and disclosures: I.Crespiatico, M.Z., C.M., D.D., M.M., C.M.M., D.F., S.S., V.C., M.G., V.S., V.B., A.A., V.C., F.B., C.B., R.O., E.A., L.M., and R.P. performed research; I.Crespiatico, C.M., D.D., M.M., C.M.M., D.F., S.S., V.C., E.I., B.M., I.Civettini, F.P., A.A., V.C., C.B., R.O., E.A., E.M.E., L.M. and R.P. collected data; I.Crespiatico, C.M., E.A., E.M.E., L.M., and R.P. analyzed and interpreted data; M.Z., E.I., B.M., I.Civettini, A.A., L.R., M.R., A.C., M.B., M.S., F.M., G.G., A.M., D.C., A.R., A.Sacco, F.S., A.Sessa, C.G-P., E.M.E., and R.P. contributed vital reagents; D.R. and R.P. contributed analytical tools and performed statistical analysis; I.Crespiatico, E.M.E., L.M., and R.P. wrote the original manuscript draft; C.M., D.F., F.P., V.S., V.C., E.A., A.Sessa, and C.G.P., reviewed and edited the manuscript; A.Sessa, C.G-P., L.M. and R.P. provided funding; A.Sessa, C.G-P., E.M.E., L.M., R.P.: supervised the study

Non-author contributions and disclosures: No;

Agreement to Share Publication-Related Data and Data Sharing Statement: The datasets supporting the conclusions of this article are available in the following SRA repositories: PRJNA795773, PRJNA793384 and PRJNA793528 BioProjects for whole-exome, whole-transcriptome and scRNA raw sequencing data, respectively.

Clinical trial registration information (if any):

Title

First-hit SETBP1 mutations cause a myeloproliferative disorder with bone marrow fibrosis.

Running head: SETBP1 induces aggressive myelofibrosis.

Authors: Ilaria Crespiatico[1]†, Mattia Zaghi[2]†, Cristina Mastini[1], Deborah D'Aliberti[1], Mario Mauri[1], Carl Mirko Mercado[1], Diletta Fontana[1], Silvia Spinelli[1], Valentina Crippa[1], Elena Inzoli[3], Beatrice Manghisi[3], Ivan Civettini[3], Daniele Ramazzotti[1], Valentina Sangiorgio[3], Michele Gengotti[1], Virginia Brambilla[4], Andrea Aroldi[1,3], Federica Banfi[2], Cristiana Barone[1], Roberto Orsenigo[5], Ludovica Riera[6], Mara Riminucci[7], Alessandro Corsi[7], Massimo Breccia[8], Alessandro Morotti[9], Daniela Cilloni[9], Aldo Roccaro[10], Antonio Sacco[10], Fabio Stagno[11], Marta Serafini[12], Federica Mottadelli[12], Giovanni Cazzaniga[1,12], Fabio Pagni[4], Roberto Chiarle[13,14,15], Emanuele Azzoni[1], Alessandro Sessa[2]*, Carlo Gambacorti-Passerini[1,3], Elena Maria Elli[3]‡, Luca Mologni[1]‡*, Rocco Piazza[1,3]‡*

Affiliations:

[1] Department of Medicine and Surgery, University of Milano-Bicocca; Monza, Italy.

[2] Neuroepigenetics Unit, Division of Neuroscience, IRCCS San Raffaele Scientific Institute; Milan, Italy.

[3] Hematology Division and Bone Marrow Unit, Fondazione IRCCS San Gerardo dei Tintori; Monza, Italy.

[4] Department of Pathology, University of Milano-Bicocca; Monza, Italy.

[5] Biomedical Research in Melanoma-Animal Models and Cancer Laboratory, Vall d'Hebron Research Institute (VHIR), Vall d'Hebron Hospital Barcelona-UAB; Barcelona, Spain.

[6] Department of Pathology, A.O.U Città della Salute e della Scienza, Turin, Italy.

[7] Department of Molecular Medicine, Az. Policlinico Umberto I, Sapienza University of Rome, Rome, Italy.

[8] Department of Translational and Precision Medicine, Az. Policlinico Umberto I, Sapienza University of Rome, Rome, Italy.

[9] Department of Clinical and Biological Sciences, University of Turin; Orbassano, Turin, Italy.

[10] Clinical Trial Center, Translational Research and Phase I Unit, ASST Spedali Civili di Brescia, Brescia, Italy.
[11] Division of Hematology, A.O.U. Policlinico "G. Rodolico-S. Marco"; Catania, Italy.
[12] Centro Tettamanti, IRCCS San Gerardo dei Tintori, Monza, Italy.
[13] Department of Molecular Biotechnology and Health Sciences, University of Torino, Italy
[14] Department of Pathology, Children's Hospital and Harvard Medical School, Boston, MA, USA
[15] European Institute of Oncology IRCCS, Division of Haematopathology, Milan, Italy

*Corresponding authors. Email: luca.mologni@unimib.it; sessa.alessandro@hsr.it; rocco.piazza@unimib.it
† Ilaria Crespiatico and Mattia Zaghi contributed equally to this work
‡ Elena Maria Elli, Luca Mologni and Rocco Piazza contributed equally to this work

Availability of data and materials

The datasets supporting the conclusions of this article are available in the following SRA repositories: PRJNA795773, PRJNA793528 and PRJNA1039582 BioProjects for whole-exome, scRNA and Cut-and-Run raw sequencing data, respectively.

Word Counts:

Text: 4399 words
Abstract: 176 words

Figure/Table Count: 6

Reference Count: 42

Scientific Category: Myeloid Neoplasia, Hematopoiesis and Stem Cells

Key Points:

- *SETBP1* mutations, acting as a first-hit/early event, drive an aggressive myelofibrosis-like myeloproliferative disorder
- *SETBP1* mutations discriminate between two subtypes of Triple-Negative Myelofibrosis, with different genetic landscape and aggressiveness.

64

65

ABSTRACT

SETBP1 mutations are found in various clonal myeloid disorders. However, it is unclear whether they can initiate leukemia, as SETBP1 mutations typically appear as later events during oncogenesis. To answer this question, we generated a mouse model expressing mutated SETBP1 in hematopoietic tissue: this model showed profound alterations in the differentiation program of hematopoietic progenitors and developed a myeloid neoplasm with megakaryocytic dysplasia, splenomegaly, and bone marrow fibrosis, prompting us to investigate *SETBP1* mutations in a cohort of 36 triple-negative primary myelofibrosis (TN-PMF) cases. We identified two distinct subgroups, one carrying SETBP1 mutations and the other completely devoid of somatic variants. Clinically, a striking difference in disease aggressiveness was noted, with SETBP1-mutated patients showing a much worse clinical course. As opposite to myelodysplastic/myeloproliferative neoplasms, where *SETBP1* mutations are mostly found as a late clonal event, single-cell clonal hierarchy reconstruction in three TN-PMF patients from our cohort revealed *SETBP1* to be a very early event, suggesting that the phenotype of the different SETBP1+ disorders may be shaped by the opposite hierarchy of the same clonal SETBP1 variants.

INTRODUCTION

Somatic *SETBP1* mutations are found in various myeloid disorders covering both myeloproliferative neoplasms (MPN) and myelodysplastic syndromes (MDS) [1–6]. What factors address SETBP1-mutated disease towards a specific phenotype is not yet understood. As *SETBP1* mutations usually coexist with additional oncogenic variants, it is possible that the combination and/or the clonal hierarchy of the different mutations may have an impact on the outcome. We and others described *SETBP1* mutations as a secondary acquisition, rather than a founding event, in leukemia progression [3–8].

SETBP1 mutations are clustered in a hotspot region controlling SETBP1 protein stability. In the past we demonstrated that mutated SETBP1 accumulates due to impaired ubiquitin-mediated degradation and stabilizes the SET oncoprotein, which inhibits the PP2A tumor suppressor [1]. In addition, SETBP1 directly regulates transcription via binding to transcriptional complexes [9,10]. Ectopic expression of mutant *SETBP1* can immortalize murine myeloid progenitors *in vitro* [11]; these progenitors are able to generate myeloid leukemia and accelerate CSF3R-driven MPN in transplanted recipient mice [12,13]. However, whether *SETBP1* mutations can initiate leukemia *in vivo* is not yet known. To answer this question, we generated a conditional mouse model that expresses SETBP1^{G870S} mutant in the entire hematopoietic tissue since embryonic life, through Cre-mediated recombination driven by the *Vav1* promoter [14,15]. The mice developed a chronic myeloid disorder with myelofibrosis, caused by an extensive subversion of the normal hematopoietic differentiation program. Intriguingly, patients diagnosed with primary myelofibrosis (PMF) lacking the classical genetic drivers were found to carry *SETBP1* mutations as the first hit, suggesting that the timing of appearance of *SETBP1* mutations along tumor history dictates the phenotype of the disease.

METHODS

Patients and study design

All patients analyzed met the diagnosis of PMF, in early or overt phase according to the WHO 2016 classification [16]. An MDS/MPN overlap syndrome diagnosis was excluded based on the presence of major and minor criteria for PMF as per WHO guidelines. Histologic examination was performed at local institution; fibrosis was graded according to the European Consensus Grading System [17]. All patients provided written informed consent approved by the institutional ethical committee (Protocol 0040864/19). The study was conducted in accordance with the Declaration of Helsinki. See Supplementary Methods for scRNA, NGS, flow cytometry and mouse model description.

RESULTS

SETBP1^{G870S} induces a myelofibrosis-like disorder in mice

To investigate the role of *SETBP1* mutations in the onset of leukemia, we generated a conditional mouse model that mimics the accumulation of mutated SETBP1 protein in bone marrow (BM) and peripheral blood (PB) cells (SETBP1^{G870S} mice; Supplementary Figure S1, S2A-B); the mouse carries a human *SETBP1-G870S* mutant gene at the Rosa26 locus that can be expressed from the artificial CAG promoter after removal of a floxed transcriptional stop. SETBP1^{G870S} pups did not show any differences in dimensions, mobility and viability compared to non-recombined (SETBP1^{LSL}) control littermates. However, in all SETBP1^{G870S} mice signs of a hematological disease appeared between 30 and 90 days after birth. Exploration of visceral organs showed massive hepatosplenomegaly (Figure 1A-C). Longitudinal analysis revealed accumulation of white blood cells (WBC) in virtually all heterozygous SETBP1^{G870S} mice (Figure 1D). Morphologic and flow cytometry analyses performed on PB showed a marked imbalance between the lymphoid and myeloid lineages in favor of the latter, with an impressive increase of mature myeloid cells and a dramatic reduction in the percentage of lymphocytes compared to controls (Figure 1E-G and

Supplementary Figure S2C-F). Unlike MDS/MPN with neutrophilia (MDS/MPNn) and related MDS/MPN disorders, no evidence of granulocytic dysplasia was noted in this mouse model. Also, no circulating blasts or non-segmented myeloid precursors were found in PB. Ultimately, 100% SETBP1^{G870S} mice succumbed of multiorgan failure due to extreme leukocytosis. Moribund mice appeared lethargic and were euthanized. Kaplan-Meier analysis revealed a dramatic decrease in Overall Survival (OS) in SETBP1^{G870S} mice (heterozygous, median survival 108 days; homozygous, 51 days) compared to SETBP1^{LSL} controls (Figure 1H). Whole-exome sequencing did not show evidence for acquisition of additional oncogenic mutations during progression (Supplementary Table S1), indicating that *SETBP1* overexpression alone is sufficient to induce a myeloproliferative phenotype.

BM histology revealed overt myeloid hyperplasia with no evidence of dysplasia except for the megakaryocytic lineage (Figure 2A-B). Atypical megakaryocytes were commonly found in SETBP1^{G870S} BM sections, with frequent hypo-lobulated bulbous nuclei, dark chromatin with irregular borders and folding of the nuclear surface. Stromal changes in terms of reticulin fibrosis were seen on BM sections taken from adult SETBP1^{G870S} mice: Gomori silver stain revealed an increased network of reticulin fibers with many intersections (average grade of fibrosis, MF-1; Supplementary Figure S2G), with a predominant peri-trabecular distribution, but also extending within the inter-trabecular spaces, as well as the presence of thick, confluent collagen fibers, while control mice showed a normal pattern (Figure 2C-D and Supplementary Figure S2H). BM cells revealed a marked expansion of lineage-negative (Lin$^-$) cells (Figure 2E-G); however, within the Lin$^-$ population, the fraction of multipotent Lin$^-$/Sca1$^+$/c-Kit$^+$ (LSK) cells was much reduced, and very few HSCs (CD150$^+$/CD48$^-$) were found in SETBP1^{G870S} BM; no significant change in the MPP3 fraction (CD150$^-$/CD48$^+$) was noted. This pattern is consistent with an amplification of committed myeloid progenitors. To better characterize myeloid progenitor populations, we analyzed Lin$^-$/Kit$^+$/Sca$^-$ (LK) cells using two pairs of surface markers, i.e., CD34/CD150 [18] and CD34/FcγR

[19]. Both analyses showed significant expansion of common myeloid progenitors (CMPs; Supplementary Figure S3) in SETBP1^{G870S} BM.

The liver and spleen of SETBP1^{G870S} mice showed marked distortion of the normal architecture (Figure 2H-K and Supplementary Figure S4). Consistent with extramedullary hematopoiesis, clusters of variably segmented myeloid cells accumulated in the liver and in the red pulp of the spleen. Flow cytometry analysis of splenocytes revealed massive infiltration by mature myeloid cells and a concomitant sharp loss of lymphoid cells in SETBP1^{G870S} mice compared with controls (Figure 2L-N) in keeping with PB data. At the same time, an aberrantly large Lin$^-$ population was found in the spleen and a significant fraction of these cells was c-Kit$^+$/Sca1$^-$, suggesting a myeloid progenitor phenotype [20].

These data indicate that mutated SETBP1 drives the development of a MPN disease characterized by myelofibrosis, megakaryocytic-restricted dysplasia, marked mature leukocytosis and progressive splenomegaly.

Mutated SETBP1 alters the transcriptional program of differentiating BM cells

Single-cell RNA-sequencing (scRNA) on BM Lin$^-$ cells from SETBP1^{G870S} and SETBP1^{LSL} mice (Figure 3A and Supplementary Figure S5A) confirmed that *SETBP1-EGFP* expression was restricted to SETBP1^{G870S} cells (Figure 3B). Analysis of differentially expressed genes (DEG) (Supplementary Table S2) identified *Setbp1*, *Hoxa9*, *Gata1*, *Gata2*, *Ezh2*, and *Mecom* among the top differential genes (Figure 3C-D, Supplementary Figure S5B-C) in the most immature myeloid population. *MECOM* and *HOXA9* are direct targets of SETBP1 transcriptional regulation [9,11]. The evidence that both genes are upregulated in our SETBP1^{G870S} model suggests that SETBP1 can modulate their expression in the context of the differentiating BM cells. *Mecom* was also shown to positively regulate endogenous *Setbp1* expression [21], suggesting that the two genes are likely co-regulated at transcriptional level, probably through a positive feedback loop. This is of particular relevance, as Mecom is known to promote expansion of the early myeloid progenitors by

suppressing the TGF-β1/Smad axis [22,23] and its overexpression has been linked to poor prognosis in myeloid malignancies [24]. In line with these findings, GSEA revealed a deep suppression of the TGF-β1 axis in SETBP1^{G870S} myeloid precursors, together with the activation of the *Hoxa9* network (Figure 3E-F, H). Interestingly, this was accompanied by a strong, positive enrichment of the Polycomb Repressor Complex 2 (PRC2) targets (Figure 3G-H), indicating that in SETBP1^{G870S} precursors the repressive activity of PRC2 was inhibited, which is a key event in myeloproliferative disorders, as opposite to acute myeloid leukemias where PRC2 activity is typically increased [25].

Western blot analyses (Figure 3I) confirmed the stabilization of the Setbp1/Set/PP2A axis [1,2] by showing accumulation of Set protein and increased PP2A phosphorylation. Overexpression of Mecom was also confirmed at protein level. In addition, we found increased expression of Bmp5 and Myc proteins [9,12] and marked phosphorylation of S6, normally associated with mitogenic stimulation [26]. Interestingly, Myc was likely upregulated post-translationally, as previously reported [27], since it was downregulated at transcriptional level. Finally, P53 protein was strongly downregulated in SETBP1^{G870S} mice, suggesting the existence of a complex SETBP1-TP53 interaction, as also noted in our previous work [28].

To investigate the mechanisms of SETBP1-driven alteration of hematopoiesis, we looked at all the spatially autocorrelated genes across the BM pseudotime for the CMP-MEP and the CMP-GMP differentiation paths (Figure 4A). We identified a total of 1686 and 1213 autocorrelated genes in the two branches (Benjamini-Hochberg-adjusted $p < 0.1$; Moran's I test > 0.15. Supplementary Tables S3-S4), with 793 genes in common between CMP-MEP and CMP-GMP. Of the 2106 autocorrelated genes globally identified in the two branches, 88.2% were also differential between SETBP1^{G870S} and SETBP1^{LSL} in the CMP/GMP/MEP clusters (Chi-Square test $p < 0.0001$; Supplementary Table S5). The fraction of spatially autocorrelated and differential genes was very high in the CMP-MEP (88.7%) as well as in the CMP-GMP (91.4%) branch, however the dysregulation of the CMP-GMP was more profound (Figure 4B-C).

As SETBP1 has been also implicated in the direct modulation of transcription as a DNA binding protein with both promoting and repressive transcriptional activity [9,11], we sought to investigate its interaction with genomic DNA in hematopoietic precursors. We performed Cut & Run experiments using Lin^- hematopoietic precursors of both $SETBP1^{G870S}$ as well as $SETBP1^{LSL}$ mice (Supplementary Tables S6-S9). Genomic DNA occupancy by SETBP1 was analyzed by using anti-SETBP1 and validated using anti-V5 antibodies. We identified a total of 1167 peaks binding to promoter regions, defined as DNA regions comprised between ±3Kb from a Transcriptional Start Site (TSS). Of them, 760 (65.1%) were also found using an anti-V5 antibody. Notably, both strategies confirmed a strong enrichment for promoters, with > 80% of the peaks consistently mapping to TSS and characterized by a broad DNA binding profile (Figure 4D-F), in line with previous ChIP-Seq experiments [9]. Of the 1167 promoter peaks, 682 (58.4%) were associated with differentially expressed genes and 233 (20.0%) were also spatially autocorrelated in the CMP/GMP/MEP differentiation branches (Figure 4G; Supplementary Table S5).

Bioprocess over-representation analysis performed on the 233 differential, autocorrelated genes directly bond by SETBP1 at promoter level (Figure 4H; Supplementary Table S10) revealed a strong enrichment of processes associated with myeloid cell differentiation (padj = $1.18*10^{-09}$), cell number homeostasis (padj = $5.4*10^{-07}$), regulation of hemopoiesis (padj = $9.5*10^{-07}$) as well as chromatin remodeling (padj = 0.03).

Among the genes modulated by the expression of mutated SETBP1, we found many critical regulators/effectors of normal hematopoiesis (Figure 4C). Specifically, a profound decrease in *Gata2* expression in $SETBP1^{G870S}$ precursors was noted (as shown in Fig. 3C-D). *Gata2* upregulates the master erythroid differentiation factor *Gata1* through a direct interaction with *Gata1* promoter, thus triggering the Gata2-to-Gata1 erythroid switch. In line with these data, *Gata1* expression was profoundly suppressed in the early myeloid precursors in $SETBP1^{G870S}$ (Fig. 3C-D; padj = 3.310^{-17}; Log_2-FC in $SETBP1^{G870S}$ *vs* $SETBP1^{LSL}$: -0.72). The expression of the Growth Factor Independent 1B zinc finger gene (*Gfi1B*), which complexes with Gata1 to promote terminal erythroid

differentiation, was also suppressed in the MEP branch (padj = $2.89*10^{-38}$; Log_2-FC in $SETBP1^{G870S}$ *vs* $SETBP1^{LSL}$: -1.0) which associated with the down-modulation of markers of erythroid and megakaryocytic lineages, such as the Carbonic Anhydrase 1 (*Car1*; Figure 4C; padj = $3.3*10^{-28}$; Log_2-FC in $SETBP1^{G870S}$ *vs* $SETBP1^{LSL}$: -1.38) or *Itga2b* (Figure 4C; padj = $2.94*10^{-88}$; Log_2-FC in $SETBP1^{G870S}$ *vs* $SETBP1^{LSL}$: -1.87).

Alteration in the transcriptional program was not restricted only to genes associated with suppression of erythroid differentiation: among the spatially autocorrelated and differentially expressed genes we also identified the myocyte enhancer factor 2C (*Mef2c*) transcription factor (Figure 4C). Mef2c is known to be a key regulator of normal megakaryopoiesis and absent or reduced MEF2C expression results in defects in megakaryocytic differentiation [29], while its upregulation has been linked to PMF and tissue fibrosis [30,31]. In $SETBP1^{G870S}$ Lin^- precursors, *Mef2c* was found to be potently upregulated in HSC (padj = $8.2*10^{-83}$; Log_2-FC: 1.22) as well as in MPP (padj = $1.86*10^{-42}$; Log_2-FC: 1.01), CMP (padj = $1.02*10^{-31}$; Log_2-FC: 1.02), GMP (padj = $1.49*10^{-53}$; Log_2-FC: 1.87) and MEP clusters (padj = $1.9*10^{-205}$; Log_2-FC: 2.77). Interestingly, Cut-&-Run experiments identified *Mef2c* as a primary Setbp1 target (Figure 4D; fold-enrichment over control: 16-fold; p = 10^{-39}), suggesting that *Mef2c* is under a direct, positive transcriptional control of Setbp1.

In parallel with a profound alteration of the megakaryocytic/erythroid axis, a concomitant activation of a group of spatially autocorrelated genes associated with stem cell potency/renewal and BM repopulation ability was noted, in particular *Zbtb16* (formerly *Plzf*), *Zbtb20*, *Tcf7*, *Ly6k*, *Ramp1* and *Slpi*. Among them, *Zbtb16*, *Zbtb20* and *Tcf7* showed a very similar pattern, with a marked upregulation in the early progenitors (Figure 4C-D).

Globally, these data suggest that expression of mutated *SETBP1* in the BM profoundly alters the differentiation program of the hematopoietic progenitors, causing a complex series of events, of which *Mecom* and *Hoxa9* activation are only a part, that are responsible for: *(a)* improving myeloid expansion and early progenitors repopulation ability; *(b)* fostering an anti-apoptotic phenotype; *(c)*

promoting the granulocytic/monocytic differentiation while suppressing erythroid and lymphoid lineages (Supplementary Figure S6).

Transplantation of SETBP1^{G870S} cells results in anemia and myeloid leukemia

In agreement with single-cell data, PB of SETBP1^{G870S} mice showed a tendency toward reduced red blood cells (RBC) and significantly lower platelet counts (Figure 5A), with concomitant expansion of white blood cells (WBC, see also Figure 1D). Anemia and thrombocytopenia were dramatically exacerbated in lethally irradiated syngeneic recipients receiving BM cells from SETBP1^{G870S} donors compared to mice receiving SETBP1^{LSL} BM (Figure 5B and Supplementary Figures S7-S8). All but one mice transplanted with SETBP1^{G870S} cells died within 16 days post-transplant due to extreme anemia. These data confirmed that SETBP1^{G870S} BM has reduced erythropoietic capacity, in line with transcriptomics analyses. It is also interesting to note that, when expressed in all tissues, mutant SETBP1 causes embryonic lethality due to reduced primitive erythropoiesis [32]. Next, as these recipients succumbed rapidly due to anemia, we turned to a sub-lethally irradiated model to allow enough time for graft expansion: donor chimerism gradually increased in recipients of SETBP1^{G870S} BM (Supplementary Figure S9A). After six weeks these mice showed mild anemia and massive leukocytosis (Figure 5C), with most cells belonging to the myeloid compartment (Supplementary Figure S9B). All transplanted mice developed an accelerated form of chronic myeloproliferation, in some cases with the presence of immature elements, that also infiltrated visceral organs (Supplementary Figure S9C-D). Mice receiving SETBP1^{G870S} cells showed reduced OS (median survival 49 days) compared with controls (Figure 5D) and with SETBP1^{G870S} donor mice ($p < 0.0001$; see also Figure 1H). Similar results were obtained by transplantation of splenocytes (Supplementary Figure S10). In line with observations in SETBP1^{G870S} BM, very few donor-derived LSK and HSCs were found in the BM of mice receiving SETBP1^{G870S} cells (Supplementary Figure S11). These data demonstrate the ability of SETBP1^{G870S} BM cells to transfer and initiate a MPN similar to the one observed in the donors, but in an accelerated form, in

recipient mice.

Paired whole-exome sequencing identifies distinct TN-PMF subgroups

The SETBP1^{G870S} mouse model recapitulated many clinical features of PMF. The molecular pathogenesis of PMF relates to mutually exclusive somatic mutations in three driver genes, *JAK2*, *CALR*, and *MPL* [33]. However, up to 10% of them are triple-negative for these mutations (TN-PMF). Hence, we set out to assess *SETBP1* mutations in the context of TN-PMF. We isolated 36 patients with a diagnosis of TN-PMF. Mutations of *JAK2*, *CALR* or *MPL* were excluded by high-depth targeted NGS panel (threshold: 1% VAF). BM sections revealed the presence of clusters of megakaryocytes, often showing hyperplasia and atypical forms. As opposite to MDS/MPNn, no evidence of dysplasia could be detected in the neutrophilic lineage. Gomori stain revealed the presence of fibrosis of grade I-III (Figure 6A-D, Supplementary Figure S12) with only 3 patients showing a grade 0. Increased granulocytic proliferation was found in the BM and no evidence of dysplasia in the granulocytic or erythroid lineages was detected. Overt evidence of leukocytosis (WBC > 25 x 10^9/L) at onset was present only in 4 cases (patients 058PMF, 007PMF, CSS7 and CSS11, with 26.3, 34.3, 48.5, and 74.8 x10^9/L leukocytes, respectively). Most of the patients presented high levels of lactate dehydrogenase (LDH). Globally, 14/36 patients fulfilled the criteria of overt PMF and 22 of prefibrotic (early) PMF, according to the WHO 2016 classification [16] (Supplementary Table S11).

Of the 36 TN-PMF patients, 30 were studied by exome sequencing and 6 by targeted sequencing: 29 of them did not reveal any significant evidence of recurrent or high VAF (> 10%) somatic mutations; in all the remaining patients (7/36; 19.4%), mutations in *SETBP1* oncogene were identified (Figure 6E and Supplementary Table S12). *SETBP1* mutations were all clustered in a narrow mutational hotspot comprised between aminoacids Asp868 and Ser871. Interestingly, both mutation Gly870Ser (patients 001PMF, 6368/17G, 20864/14G and CSS7) and mutation Asp868Asn

(patients 007PMF, 037PMF and CSS8) have been previously identified by our team and by others in different myeloid disorders [1,34].

In all TN-PMF cases mentioned above, *SETBP1* mutations were detected at high VAF (> 30%). In patients 001PMF and CSS8, *SETBP1* mutation coexisted with activating *NRAS* mutations p.Gly12Ser and p.Gly13Asp, respectively; in patient 007PMF, *SETBP1* was found together with somatic *TET2* nonsense mutation p.Gln891*, with *SRSF2* p.Pro95Leu and with *RIT1* p. Phe82Leu, and in patient 037PMF with *SRSF2* p.Pro95Leu, *ASXL1* p.Arg404* and *CBL* p.Tyr368Cys. Notably, mutations of *SETBP1* were the only shared alteration among all seven patients.

Therefore, our study suggests a clear partition of TN-PMF into two groups, the first one characterized by oncogenic, high VAF *SETBP1* mutations accompanied by other oncogenic variants (hereafter referred to as SETBP1 positive group) and the other one characterized by no evidence of an active clonal process or of driver oncogenic events (SETBP1 negative group).

Clinical characteristics of SETBP1-positive and negative TN-PMF

Median age at onset (72.2 *vs* 69 years; p = 0.26), hemoglobin levels (131 *vs* 120 g/L; p = 0.78) and platelet counts (428 *vs* 448 $x10^9$/L; p = 0.55) were similar in SETBP1 positive and negative groups (Supplementary Table S11). Median WBC values at onset showed a trend towards higher counts in the SETBP1 positive group (16.4 *vs* 8.3 $x10^9$/L, p = 0.072). No difference was observed between the two groups at diagnosis in terms of BM fibrosis, IPSS score, LDH level, blast counts or spleen size. By contrast, SETBP1 positive patients showed a worse clinical course: after a median follow-up of 60 months, we reported 6 deaths, 4 of them in SETBP1 positive (4/7; 57.1%) and 2 in SETBP1 negative patients (2/29; 6.9% - Supplementary Table S11). A markedly reduced overall survival was observed for SETBP1 positive patients, with a median survival time of 24 months (Figure 6F; Kaplan-Meier Log-rank test p = 0.0017). Principal causes of death were severe infection and disease progression.

Median WBC values at 3 years from diagnosis were 100.0 *vs* 7.14 x10^9/L in SETBP1 positive and negative group, respectively ($p < 0.0001$). Progressive splenomegaly on ultrasound (16.0 *vs* 12.0 cm; $p = 0.026$), lower hemoglobin levels (72 *vs* 132 g/L; $p = 0.0049$) and a trend towards a lower platelet count (73 *vs* 471 x10^9/L; $p = 0.0598$) became also evident in the SETBP1 positive group. We assessed the association of 8 meaningful clinical and genetic variables at onset (age, gender, BM fibrosis, hemoglobin, WBC, platelets, thrombosis, *SETBP1* mutation) with overall survival, by a regularized Cox regression analysis, in 33 patients for whom these data were available. This multivariate analysis selected the presence of *SETBP1* mutation as the variable most strongly associated with poor survival (Supplementary Table S13).

SETBP1 mutation is an early event in TN-PMF

As *SETBP1* mutations found in TN-PMF are virtually identical to those found in MDS/MPN, they cannot explain the phenotypical differences of the two disorders. As several works recently highlighted a critical role for clonal hierarchy in shaping the precise phenotype and clinical aggressiveness of tumors [35,36] and since *SETBP1* was found to be mostly a secondary event in MDS/MPN neoplasms [7,8], we hypothesized that the diverging phenotype could be explained by a different clonal architecture.

To dissect the clonal architecture of SETBP1 positive TN-PMF at single-cell resolution, we applied single-cell targeted DNA sequencing on 3 SETBP1-mutated TN-PMF samples using the Tapestri technology. In all cases *SETBP1* was found to be a very early event (Figure 6G-I). Interestingly, in two out of three cases, we also isolated a late clone characterized by the presence of homozygous *SETBP1* mutations. This could be relevant, as a recent work reported the identification of clones with homozygous *SETBP1* variants in advanced, therapy resistant juvenile myelomonocytic leukemia [37]. If confirmed in larger cohorts, these data suggest that heterozygous *SETBP1* mutations occur very early in TN-PMF, while the presence of homozygous *SETBP1* variants could be the hallmark of a more aggressive, late-stage disorder. To test this hypothesis, we characterized the

homozygous hematopoietic SETBP1^{G870S} model. Compared to their heterozygous littermates, homozygous mice developed myeloid disease with shorter latency and had dramatically decreased OS (see Figure 1H). PB analysis revealed massive neutrophilia and lymphopenia already evident at 30 days of age (Figure 6J), confirming a more aggressive disorder in homozygous SETBP1^{G807S} mice compared to the heterozygous. Consistently, PB smears showed the presence of an expanded population of mature neutrophils and almost complete absence of lymphocytes (Figure 6K). In approximately 20% of homozygous SETBP1^{G807S} mice we noted, at autopsy, the presence of extramedullary masses of myeloid blasts, suggesting the progression to an acute leukemia (Supplementary Figure S13).

DISCUSSION

The involvement of *SETBP1* in myeloid transformation is supported by several studies describing recurrent *SETBP1* mutations in different clinical subtypes of myeloid malignancy [1,3,4,6,38]. Previous studies have shown that *Setbp1* overexpression confers self-renewal capability to myeloid progenitors *in vitro* and promotes acute leukemia in transplanted mice [13]. These data suggest that *Setbp1* has transforming ability but do not clarify the observation that in humans *SETBP1* is often associated with chronic myeloproliferative disorders. Here, the central role of mutated *SETBP1* in the phenotype of SETBP1 positive diseases is reinforced by the striking phenotype of the Vav-SETBP1 mouse model, which develops a chronic MPN and provides new insights into the leukemogenic role of Setbp1 *in vivo*, specifically pointing to a profound Setbp1-driven alteration of the hematopoietic differentiation programs. As *Gata2* expression is critical for the normal differentiation of the megakaryocyte lineage and its heterozygous loss-of-function causes a dysplastic megakaryocyte/platelet phenotype, its strong downregulation in SETBP1^{G870S} may explain the presence of abnormal megakaryocytes in the BM of mice. Similarly, alteration of master genes involved in the myeloid and erythroid/megakaryocytic differentiation branches, such as

386 *Mef2C*, *Mecom* and *Gata1*, further supports this notion. In particular, *Mef2C* is strongly upregulated
387 in SETBP1^{G870S}; Cut-&-Run experiments carried out in Lin$^-$ bone marrow precursors clearly
388 showed that its promoter is occupied by SETBP1: this suggests a direct control exerted by the
389 oncogene over Mef2c expression. As Mef2C overexpression has been linked to PMF and tissue
390 fibrosis, these findings may highlight for the first time a direct connection between SETBP1-
391 mutated disorders and myelofibrosis.
392 The Vav-SETBP1 mouse model precisely recapitulates WHO diagnostic criteria for PMF, including
393 some aspects that are not commonly observed in MDS/MPN disorders, such as BM fibrosis,
394 hepatosplenomegaly and megakaryocytic dysplasia. Although our murine model closely mimics the
395 phenotype of the human counterpart, it is important to note that it also has a limitation: as transgene
396 expression is driven by a strong promoter, it is hard to discriminate between the effects of the
397 mutation and those of SETBP1 over-expression.
398 Here we identified two clearly distinct subgroups within TN-PMF patients, according to the
399 presence or absence of somatic mutations of *SETBP1* and other known oncogenes. Importantly, a
400 sharp difference in disease aggressiveness was noted between the two groups, with SETBP1-
401 mutated patients showing a much worse clinical course and severe prognosis, indicating that
402 SETBP1-mutated TN-PMF patients may represent a distinct subgroup of clinically aggressive PMF.
403 Thus, SETBP1 positive diseases could possibly benefit from a more aggressive clinical approach
404 including also early hematopoietic stem cells transplantation. On the contrary, SETBP1 negative
405 patients could be spared from aggressive and toxic approaches, given its benign clinical course.
406 In the past, Leborde and colleagues reported *SETBP1* to be rarely mutated in PMF cases [42]; in their
407 study, however, *SETBP1* variants were analyzed in the context of the entire PMF cohort, with no
408 selection of TN cases. These data indicate that *SETBP1* mutations are exceedingly rare in driver-
409 positive PMF, but they are highly recurrent in TN-PMF, with SETBP1-mutated TN-PMF patients
410 showing distinctive characteristics, such as BM fibrosis with megakaryocytic dysplasia,
411 extramedullary hematopoiesis, and significant splenomegaly. Taken globally, our data indicate that

SETBP1 positive TN-PMF disorders lie in a gray zone comprised between the MPN and MPN/MDS boundary, where *SETBP1* mutations are frequently found. However, in MDS/MPN, *SETBP1* mutations are known to be late events in the history of the neoplasm. In contrast, we show here that in TN-PMF *SETBP1* is one of the earliest hits, therefore highlighting a potentially relevant biological differences occurring in the two subsets. In this context the presence of early, high VAF *SETBP1* mutations seems to promote the occurrence of a myeloid disorder characterized by the triad: leukocytosis without differentiation block or dysplasia, BM fibrosis and progressive splenomegaly, hence recapitulating many clinical features of PMF. Interestingly, in the context of single-cell clonal architecture reconstruction, we also identified the presence of late subclones carrying homozygous SETBP1 degron variants. This finding suggests that the presence of homozygous *SETBP1* variants could be associated with a more aggressive phenotype and may represent the hallmark of the late stage of SETBP1 positive TN-PMF disorders.

In conclusion, we show that the $SETBP1^{G870S}$ mouse model, without the cooperation of other clonal mutations, recapitulates all the aggressive clinical features induced by SETBP1 in humans. As the prognosis of the SETBP1-driven disorders, among them TN-PMF and MDS/MPN, is still dismal, a significant effort should be dedicated in the next future to the development of new drugs for the treatment of the *SETBP1* spectrum, which can now also rely on the availability of our *in vivo* model, which represents a novel platform for the exploration of new therapeutic approaches. Our data suggest that *SETBP1* oncogenic mutations are certainly necessary, although perhaps not sufficient, to confer aggressiveness to the disease. A larger cohort of patients will need to be analyzed to confirm these findings.

Acknowledgements

We wish to thank all patients who participated in the trial and medical as well as technical staff of participating centers. This work was supported by: Italian Association for Cancer Research (AIRC) grant IG-22082 (RP), Italian Association for Cancer Research (AIRC) grant IG-24828 (LM), Italian Association for Cancer Research (AIRC) grant IG-20112 (CG-P), Italian Ministry of University and Research (MIUR) - Department of Excellence project PREMIA (PREcision MedIcine Approach: bringing biomarker research to the clinic) (RP), Italian MUR Dipartimenti di Eccellenza 2023-2027 (l. 232/2016, art. 1, commi 314 - 337) (RP), European Union - NextGenerationEU through the Italian Ministry of University and Research under PNRR - M4C2-I1.3 Project PE_00000019 "HEAL ITALIA" (RP), European Joint Programme for Rare Diseases ERARE 2020 (RP, ASe), Fondazione Cariplo grant 2018-0102 (EA), Leukemia Research Foundation award 831382 (EA)

446 **Authorship Contributions**

447 IC: Performed research; analyzed and interpreted data; wrote the manuscript

448 MZ: Performed research; contributed vital reagents

449 CM: Performed research

450 DD: Performed research

451 MM: Performed research

452 CMM: Performed research

453 DF: Performed research; revised the manuscript

454 SS: Performed research

455 VC: Performed research; revised the manuscript

456 EI: Collected data

457 BM: Collected data

458 IC: Collected data

459 DR: Analyzed and interpreted data

460 VS: Analyzed and interpreted data

461 MG: Collected data

462 VB: Performed research

463 AA: Performed research

464 FB: Performed research

465 CB: Performed research

466 RO: Performed research

467 LR: Contributed vital new reagents; collected data

468 MR: Contributed vital new reagents; analyzed and interpreted data

469 AC: Contributed vital new reagents; analyzed and interpreted data

470 MB: Contributed vital new reagents; collected data

471 AM: Contributed vital new reagents; analyzed and interpreted data

DC: Contributed vital new reagents

AR: Contributed vital new reagents; collected data

AS: Contributed vital new reagents; collected data

FS: Contributed vital new reagents; collected data

MS: Analyzed and interpreted data

FM: Analyzed and interpreted data

GC: Analyzed and interpreted data

FP: Analyzed and interpreted data

RC: Contributed vital new reagents; collected data; analyzed and interpreted data

EA: Performed research; analyzed and interpreted data

AS: Contributed vital new reagents; analyzed and interpreted data; critically revised the manuscript

CGP: Analyzed and interpreted data; critically revised the manuscript

EME: Contributed vital new reagents; designed research; analyzed and interpreted data; critically revised the manuscript

LM: Contributed vital new reagents; designed research; analyzed and interpreted data; wrote the manuscript

RP: Contributed vital new reagents; designed research; analyzed and interpreted data, wrote the manuscript

Disclosure of Conflicts of Interest

The authors have no conflicts of interest to declare.

References

1. Piazza R, Valletta S, Winkelmann N, et al. Recurrent SETBP1 mutations in atypical chronic myeloid leukemia. *Nat. Genet.* 2013;45:18–24.
2. Cristóbal I, Blanco FJ, Garcia-Orti L, et al. SETBP1 overexpression is a novel leukemogenic mechanism that predicts adverse outcome in elderly patients with acute myeloid leukemia. *Blood*. 2010;115(3):615–625.
3. Sakaguchi H, Okuno Y, Muramatsu H, et al. Exome sequencing identifies secondary mutations of SETBP1 and JAK3 in juvenile myelomonocytic leukemia. *Nat. Genet.* 2013;45(8):937–941.
4. Makishima H, Yoshida K, Nguyen N, et al. Somatic SETBP1 mutations in myeloid malignancies. *Nat. Genet.* 2013;45(8):942–946.
5. Elliott MA, Pardanani A, Hanson CA, et al. ASXL1 mutations are frequent and prognostically detrimental in CSF3R-mutated chronic neutrophilic leukemia. *Am. J. Hematol.* 2015;90(7):653–656.
6. Damm F, Itzykson R, Kosmider O, et al. SETBP1 mutations in 658 patients with myelodysplastic syndromes, chronic myelomonocytic leukemia and secondary acute myeloid leukemias. *Leukemia*. 2013;27(6):1401–1403.
7. Fontana D, Ramazzotti D, Aroldi A, et al. Integrated Genomic, Functional, and Prognostic Characterization of Atypical Chronic Myeloid Leukemia. *HemaSphere*. 2020;4(6):e497.
8. Makishima H. Somatic SETBP1 mutations in myeloid neoplasms. *Int. J. Hematol.* 2017;105(6):732–742.
9. Piazza R, Magistroni V, Redaelli S, et al. SETBP1 induces transcription of a network of development genes by acting as an epigenetic hub. *Nat Commun*. 2018;9(1):2192.
10. Nguyen N, Gudmundsson KO, Soltis AR, et al. Recruitment of MLL1 complex is essential for SETBP1 to induce myeloid transformation. *iScience*. 2022;25(1):103679.
11. Oakley K, Han Y, Vishwakarma BA, et al. Setbp1 promotes the self-renewal of murine

myeloid progenitors via activation of Hoxa9 and Hoxa10. *Blood*. 2012;119(25):6099–6108.

12. Carratt SA, Kong GL, Curtiss BM, et al. Mutated SETBP1 activates transcription of Myc programs to accelerate CSF3R-driven myeloproliferative neoplasms. *Blood*. 2022;140(6):644–658.

13. Vishwakarma BA, Nguyen N, Makishima H, et al. Runx1 repression by histone deacetylation is critical for Setbp1-induced mouse myeloid leukemia development. *Leukemia*. 2016;30:200–208.

14. Neo WH, Booth CAG, Azzoni E, et al. Cell-extrinsic hematopoietic impact of Ezh2 inactivation in fetal liver endothelial cells. *Blood*. 2018;131(20):2223–2234.

15. Siegemund S, Shepherd J, Xiao C, Sauer K. hCD2-iCre and Vav-iCre mediated gene recombination patterns in murine hematopoietic cells. *PLoS One*. 2015;10(4):e0124661.

16. Arber DA, Orazi A, Hasserjian R, et al. The 2016 revision to the World Health Organization classification of myeloid neoplasms and acute leukemia. *Blood*. 2016;127(20):2391–2405.

17. Gianelli U, Vener C, Bossi A, et al. The European Consensus on grading of bone marrow fibrosis allows a better prognostication of patients with primary myelofibrosis. *Mod Pathol*. 2012;25:1193–1202.

18. Olender L, Thapa R, Gazit R. Isolation of Murine Myeloid Progenitor Populations by CD34/CD150 Surface Markers. *Cells*. 2022;11(3):.

19. Akashi K, Traver D, Miyamoto T, Weissman IL. A clonogenic common myeloid progenitor that gives rise to all myeloid lineages. *Nature*. 2000;404(6774):193–197.

20. Aurrand-Lions M, Mancini SJC. Murine Bone Marrow Niches from Hematopoietic Stem Cells to B Cells. *Int. J. Mol. Sci.* 2018;19(8):2353.

21. Goyama S, Yamamoto G, Shimabe M, et al. Evi-1 is a critical regulator for hematopoietic stem cells and transformed leukemic cells. *Cell Stem Cell*. 2008;3:207–220.

22. Alliston T, Ko TC, Cao Y, et al. Repression of bone morphogenetic protein and activin-inducible transcription by Evi-1. *J. Biol. Chem.* 2005;280(25):24227–24237.

23. Wang X, Dong F, Zhang S, et al. TGF-β1 Negatively Regulates the Number and Function of Hematopoietic Stem Cells. *Stem cell reports*. 2018;11(1):274–287.
24. Sayadi A, Jeyakani J, Seet SH, et al. Functional features of EVI1 and EVI1Δ324 isoforms of MECOM gene in genome-wide transcription regulation and oncogenicity. *Oncogene*. 2016;35(18):2311–2321.
25. Iwama A. Polycomb repressive complexes in hematological malignancies. *Blood*. 2017;130(1):23–29.
26. Biever A, Valjent E, Puighermanal E. Ribosomal Protein S6 Phosphorylation in the Nervous System: From Regulation to Function. *Front. Mol. Neurosci.* 2015;8:75.
27. Farrell AS, Sears RC. MYC degradation. *Cold Spring Harb. Perspect. Med.* 2014;4(3):.
28. Banfi F, Rubio A, Zaghi M, et al. SETBP1 accumulation induces P53 inhibition and genotoxic stress in neural progenitors underlying neurodegeneration in Schinzel-Giedion syndrome. *Nat. Commun.* 2021;12(1):4050.
29. Kong X, Ma L, Chen E, Shaw CA, Edelstein LC. Identification of the Regulatory Elements and Target Genes of Megakaryopoietic Transcription Factor MEF2C. *Thromb. Haemost.* 2019;119(5):716–725.
30. Norfo R, Zini R, Pennucci V, et al. miRNA-mRNA integrative analysis in primary myelofibrosis CD34+ cells: role of miR-155/JARID2 axis in abnormal megakaryopoiesis. *Blood*. 2014;124(13):e21-32.
31. Zhang W, Ping J, Zhou Y, Chen G, Xu L. Salvianolic Acid B Inhibits Activation of Human Primary Hepatic Stellate Cells Through Downregulation of the Myocyte Enhancer Factor 2 Signaling Pathway. *Front. Pharmacol.* 2019;10:322.
32. Zaghi M, Banfi F, Massimino L, et al. Balanced SET levels favor the correct enhancer repertoire during cell fate acquisition. *Nat. Commun.* 2023;in press:
33. Tefferi A, Nicolosi M, Mudireddy M, et al. Driver mutations and prognosis in primary myelofibrosis: Mayo-Careggi MPN alliance study of 1,095 patients. *Am. J. Hematol.*

2018;93(3):348–355.

34. Acuna-Hidalgo R, Deriziotis P, Steehouwer M, et al. Overlapping SETBP1 gain-of-function mutations in Schinzel-Giedion syndrome and hematologic malignancies. *PLoS Genet*. 2017;13:e1006683.

35. Ortmann CA, Kent DG, Nangalia J, et al. Effect of mutation order on myeloproliferative neoplasms. *N. Engl. J. Med.* 2015;372(7):601–612.

36. Nangalia J, Nice FL, Wedge DC, et al. DNMT3A mutations occur early or late in patients with myeloproliferative neoplasms and mutation order influences phenotype. *Haematologica*. 2015;100(11):e438-42.

37. Stieglitz E, Troup CB, Gelston LC, et al. Subclonal mutations in SETBP1 confer a poor prognosis in juvenile myelomonocytic leukemia. *Blood*. 2015;125(3):516–524.

38. Gotlib J, Maxson JE, George TI, Tyner JW. The new genetics of chronic neutrophilic leukemia and atypical CML: implications for diagnosis and treatment. *Blood*. 2013;122:1707–1711.

39. Sahoo SS, Kozyra EJ, Wlodarski MW. Germline predisposition in myeloid neoplasms: Unique genetic and clinical features of GATA2 deficiency and SAMD9/SAMD9L syndromes. *Best Pract. Res. Clin. Haematol.* 2020;33(3):101197.

40. McReynolds LJ, Calvo KR, Holland SM. Germline GATA2 Mutation and Bone Marrow Failure. *Hematol. Oncol. Clin. North Am.* 2018;32(4):713–728.

41. Fisher KE, Hsu AP, Williams CL, et al. Somatic mutations in children with GATA2-associated myelodysplastic syndrome who lack other features of GATA2 deficiency. *Blood Adv.* 2017;1(7):443–448.

42. Laborde RR, Patnaik MM, Lasho TL, et al. SETBP1 mutations in 415 patients with primary myelofibrosis or chronic myelomonocytic leukemia: independent prognostic impact in CMML. *Leukemia*. 2013;27(10):2100–2102.

43. Dorsam ST, Ferrell CM, Dorsam GP, et al. The transcriptome of the leukemogenic

599 homeoprotein HOXA9 in human hematopoietic cells. *Blood*. 2004;103(5):1676–1684.

600

Figure Legends:

Figure 1. Phenotype of the SETBP1^{G870S} mouse. (A) Gross examination of SETBP1^{LSL} (first panel) and SETBP1^{G870S} (second and third panel) mice at autopsy, showing massive enlargement of spleen and liver in SETBP1^{G870S} mice (red arrows). The fourth panel shows the spleen of SETBP1^{LSL} (left) and SETBP1^{G870S} mouse (right); the red arrow points to a splenic infarction occurring in SETBP1^{G870S}. **(B-C)** Spleen size (B) and weight (C) of SETBP1^{LSL} (green) and SETBP1^{G870S} (orange) mice, confirming massive spleen enlargement. Statistical analysis was performed using a two-tailed t-test. **(D)** Total WBC counts reported over the course of a 150 days follow-up for SETBP1^{G870S} (orange) and SETBP1^{LSL} (green) mice. **(E)** H&E stained PB cytospins of a 60 days SETBP1^{G870S} mouse showing accumulation of mostly mature neutrophils with less abundant monocytes. **(F)** Violin plot showing the fraction of myeloid cells over the total WBC count in SETBP1^{LSL} (green) and SETBP1^{G870S} (orange) mice at 120 days, as determined by pathologist's counts on cytospin slides. Statistical analysis was performed using a two-tailed t-test. **(G)** (*left*) FACS analysis of representative SETBP1^{LSL} (green) and SETBP1^{G870S} (orange) PBMCs; CD11b *vs* Ly6G (upper) and CD3 *vs* GFP (lower) plots are shown, displaying massive expansion of CD11b^{+} myeloid cells and dramatic reduction of CD3^{+} lymphocytes. Blood samples were collected at 120 days; (*right*) aggregated FACS data (n = 6). **(H)** Kaplan-Meier OS analysis. P-values were calculated with the use of a log-rank test and mice were stratified according to their genotype (SETBP1^{G870S}, heterozygous, orange; SETBP1^{G870S}, homozygous, red; SETBP1^{LSL}, green). Tick marks indicate censored data.

Figure 2. Pathology of SETBP1^{G870S} mouse. (A-B) Hematoxylin-Eosin (H&E) staining of age-matched (3 months) SETBP1^{LSL} (A) and SETBP1^{G870S} (B) bone marrow (scale bars 25 µm). In controls, BM sections showed a normal granulocytes segmentation with mature poly-lobulated megakaryocytes. In diseased mice, myeloid differentiation was abnormally shifted to the left and frequent atypical megakaryocytes were seen (black arrows). **(C-D)** BM sections stained with a Gomori silver stain in a SETBP1^{LSL} (C) and a SETBP1^{G870S} (D) mouse at 150 days of age (scale bar 25 µm). An increased network of reticulin fibers with many intersections can be noted in SETBP1^{G870S}. The red arrows point to thick, confluent fibers. Control BM shows normal reticulin structure; the small arrow points to normal perivascular staining as an internal positive control. **(E-F)** FACS analysis of BM cells from representative SETBP1^{LSL} (E) and SETBP1^{G870S} (F) mice. CD45^{+} cells were stained with myeloid, lymphoid and stem cell markers, as indicated. (**G**) Aggregated data from FACS analysis of BM samples (n = 5). **(H-K)** H&E stained histological sections of liver (H-I; scale bars 25 µm) and spleen (J-K; scale bars 100 µm) on SETBP1^{LSL} (H, J) and SETBP1^{G870S} (I, K) mice. In both organs, SETBP1^{G870S} mice showed subversion of the normal parenchyma with accumulation of myeloid cells and evidence of extramedullary hematopoiesis. Clusters of myeloid elements were present in the liver, with peri-portal distribution. Red pulp colonization in the spleen showed clusters of abnormal megakaryocytes with hyper-condensed chromatin; also, numerous bare megakaryocytic nuclei were present. **(L-M)** FACS analysis of spleen cells from SETBP1^{LSL} (L) and SETBP1^{G870S} (M) mice. CD45^{+} cells were stained with myeloid, lymphoid and progenitor cell markers, as indicated. (**N**) Aggregated data from FACS analysis of splenocytes (n = 5).

Figure 3. Single-cell transcriptome analysis of SETBP1^{LSL} and SETBP1^{G870S} Lin$^-$ bone marrow cells. (A) UMAP plot showing the integrated scRNA analysis, color-coded by cell type. HSC: Hematopoietic Stem Cells; ETP: Earliest Thymic Progenitors; T-DN2a: T-DN2a cells; CMP: Common Myeloid Progenitors; GMP: Granulocyte-Monocyte Progenitors; MEP: Megakaryocytic-Erythroid Progenitors; CDP: Common Dendritic Progenitors; MDP: Monocyte-Dendritic cell Progenitors; Tem: T Effector Memory cells; DC: Dendritic cells. **(B)** UMAP plot reporting the expression level of the artificial SETBP1-EGFP transcript in SETBP1^{LSL} *(left)* and SETBP1^{G870S} *(right)* 90-days old littermates in a blue-to-yellow color-scale. **(C)** UMAP plots reporting the expression level of *Setbp1*, *Gata2*, *Hoxa9*, *Ezh2* and *Gata1* in SETBP1^{LSL} *(left)* and SETBP1^{G870S} *(right)* mice in a blue-to-yellow color-scale. **(D)** Violin plot showing the expression level of *Setbp1*, *Gata2*, *Hoxa9*, *Ezh2* in the HSC cluster and of *Gata1* in the CMP cell cluster of SETBP1^{LSL} (green) and SETBP1^{G870S} (orange) mice. Differentially expressed genes were identified using a negative binomial generalized linear model; the false-positive discovery rate was controlled using the Bonferroni procedure. **(E,F,G)** Enriched gene-sets for *TGF-Beta Signaling*, *Hoxa9 downregulated targets* and *PRC2 targets* identified in in SETBP1^{G870S} *vs* SETBP1^{LSL} HSC cells. FDR represents the Benjamini-Hochberg adjusted p-value; NES is the Normalized GSEA enrichment score. *HOXA 9_TARGETS_DN* represents genes that are down-regulated in hematopoietic stem cells expressing *HOXA9* [43]. **(H)** Heatmap of the top GSEA leading edge genes of the *TGF-Beta Signaling*, *Hoxa9 downregulated targets* and *PRC2 targets* pathways in SETBP1^{LSL} (*left*, green ribbon) and SETBP1^{G870S} (*right*, orange ribbon) mice. **(I)** Western blot analysis of PB samples obtained from SETBP1^{LSL} and SETBP1^{G870S} mice; transgenic SETBP1 is detected both by anti-SETBP1 and anti-V5 antibodies. Actin is shown as a loading control.

Figure 4. Single-cell analysis of SETBP1^{LSL} and SETBP1^{G870S} bone marrow cells. (A) Left: UMAP projection of the full, integrated SETBP1^{G870S}/SETBP1^{LSL} single-cell analysis, annotated with cell type. The orange area highlights the HSC, CMP, GMP and MEP cell populations. Right: UMAP projection of the HSC, CMP, GMP and MEP cell populations. The grey line represents the pseudotime path. **(B)** Gene expression heatmap of autocorrelated genes from root to fate in the CMP to MEP (upper panel) and CMP to GMP (lower panel) trajectories for SETBP1^{LSL} (left) and SETBP1^{G870S} (right) cells. **(C)** UMAP plots reporting the expression level of a subset of differentially expressed and autocorrelated genes in a blue-to-yellow color-scale. Orange dots identify genes that are differentially expressed in SETBP1^{G870S} *vs* SETBP1^{LSL}; blue and green dots highlight genes that are spatially autocorrelated in the CMP-MEP and CMP-GMP trajectories, respectively; red dots identify genes that represent direct transcriptional SETBP1 targets. **(D)** Alignment plots of *Hoxa9/10*, *Mecom*, *Mef2c* and *Zbtb20* loci for anti-SETBP1 Cut & Run experiments performed in Lin$^-$ bone marrow cells of SETBP1^{G870S} and SETBP1^{LSL} mice models. **(E)** Cumulative distribution of SETBP1 and V5 binding loci relative to Transcription Start Site (TSS). **(F)** Heatmap of anti-SETBP1 Cut & Run reads binding to TSS. **(G)** Venn diagram showing the intersection between DEGs identified in SETBP1$^{G870S\ vs}$ SETBP1^{LSL} in CMP, GMP and MEP clusters, spatially autocorrelated genes in CMP to MEP and CMP to GMP trajectories and peaks identified in Cut & Run experiments using an anti-SETBP1 antibody. **(H)** Biological process over-representation analysis performed using the intersection of DEGs identified in SETBP1$^{G870S\ vs}$ SETBP1^{LSL} in CMP, GMP, and MEP clusters, spatially autocorrelated genes in CMP to MEP and CMP to GMP trajectories and peaks identified in Cut & Run experiments as input. The FDR is reported in a blue-to-red color-scale.

690 **Figure 5. Whole BM transplantation in recipient mice.** RBC, platelets (PLT) and WBC counts in
691 the PB of: **(A)** adult SETBP1^{LSL} and SETBP1^{G870S} mice; **(B)** lethally irradiated secondary recipients
692 of SETBP1^{LSL} and SETBP1^{G870S} BM, 2 weeks after transplant; **(C)** sub-lethally irradiated recipients
693 of SETBP1^{LSL} and SETBP1^{G870S} BM, 6 weeks after transplant. Blood cell counts were obtained
694 using a blood analyzer; **(D)** OS of sub-lethally irradiated recipients of SETBP1^{G870S} BM (orange)
695 and SETBP1^{LSL} BM (green).

Figure 6. Molecular and clinical characteristics of Triple-Negative Primary Myelofibrosis patients. (A-D) Representative BM seriated sections from two TN-PMF patients stained with H&E **(**A and C) and reticulin stain (B and D). Fibrosis with osteomyelosclerosis and megakaryocyte hyperplasia (with cluster formation and atypical forms) associated with fibrosis grade 3 are shown in panels A and B and in panels C and D, respectively. Bars: 500 µm in A and B and 200 µm in C and D. **(E)** Oncoprint reporting the somatic mutations identified in the TN-PMF cohort. The orange and green bars highlight the SETBP1-positive and negative patients, respectively. **(F)** Kaplan-Meier survival analysis. TN-PMF patients were stratified according to the somatic mutational burden, with SETBP1 positive cases shown in orange and SETBP1 negative patients in green. The log-rank test was used to test for differences in survival between the two groups. Tick marks indicate censored data. **(G-I)** Fish plots showing somatic evolution of the disease in three TN-PMF patients. In two cases (G, I), a late acquisition of homozygous SETBP1 mutation is observed. **(J)** Neutrophil and lymphocyte populations in PB from homozygous (homo) and heterozygous (het) $SETBP1^{G870S}$ mice. **(K)** H&E staining of PB from a 30-days homozygous $SETBP1^{G870S}$ mouse showing accumulation of mature granulocytes.

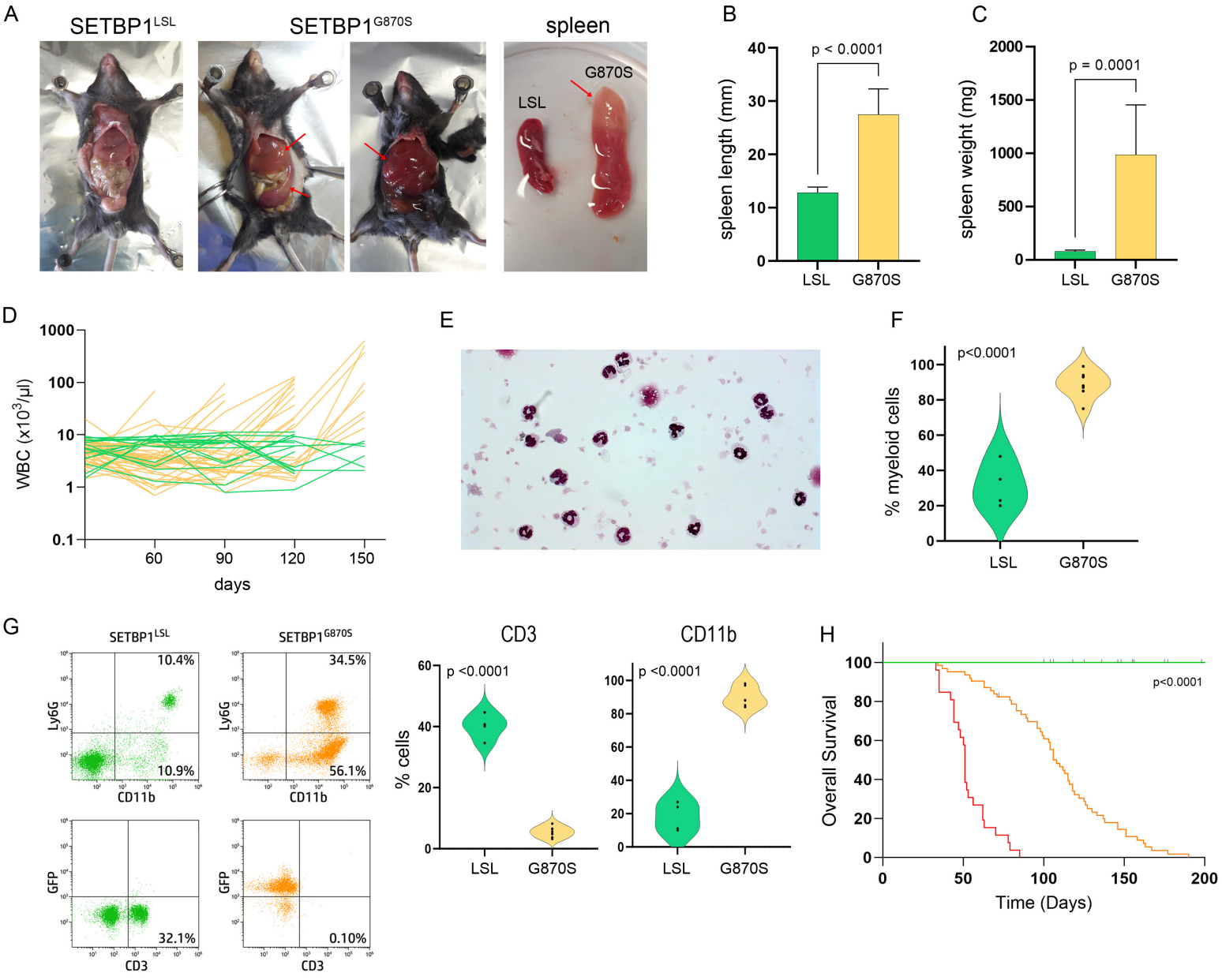
A
SETBP1LSL
SETBP1G870S
spleen
G870S
LSL
B
p < 0.0001
spleen length (mm)
LSL
G870S
C
p = 0.0001
spleen weight (mg)
LSL
G870S
D
WBC (x10³/µl)
days
E
F
p<0.0001
% myeloid cells
LSL
G870S
G
SETBP1LSL
SETBP1G870S
10.4%
10.9%
34.5%
56.1%
Ly6G
CD11b
GFP
CD3
32.1%
0.10%
CD3
p <0.0001
% cells
LSL
G870S
CD11b
p <0.0001
LSL
G870S
H
p<0.0001
Overall Survival
Time (Days)

Figure 2

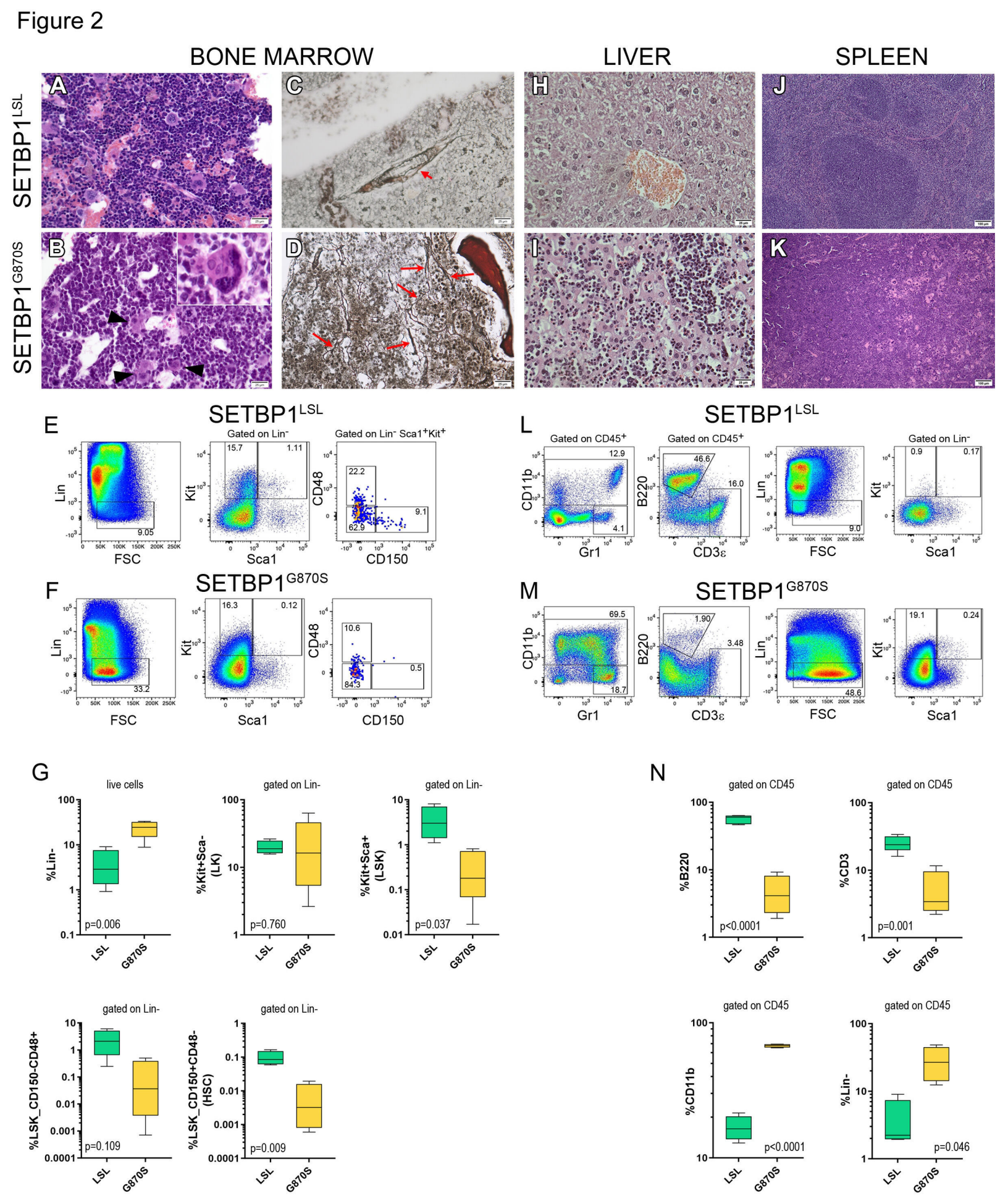
BONE MARROW
LIVER
SPLEEN
SETBP1LSL
SETBP1G870S
A
B
C
D
H
I
J
K
E
SETBP1LSL
Gated on Lin-
Gated on Lin- Sca1+Kit+
Lin
FSC
9.05
Kit
Sca1
15.7
1.11
CD48
CD150
22.2
9.1
62.9
F
SETBP1G870S
16.3
0.12
33.2
10.6
0.5
84.3
L
SETBP1LSL
Gated on CD45+
CD11b
Gr1
12.9
4.1
B220
CD3ε
46.6
16.0
Gated on Lin-
9.0
0.9
0.17
M
SETBP1G870S
69.5
18.7
1.90
3.48
19.1
0.24
48.6
G
live cells
%Lin-
p=0.006
LSL
G870S
gated on Lin-
%Kit+Sca- (LK)
p=0.760
%Kit+Sca+ (LSK)
p=0.037
%LSK_CD150-CD48+
p=0.109
%LSK_CD150+CD48- (HSC)
p=0.009
N
gated on CD45
%B220
p<0.0001
%CD3
p=0.001
%CD11b
p<0.0001
%Lin-
p=0.046

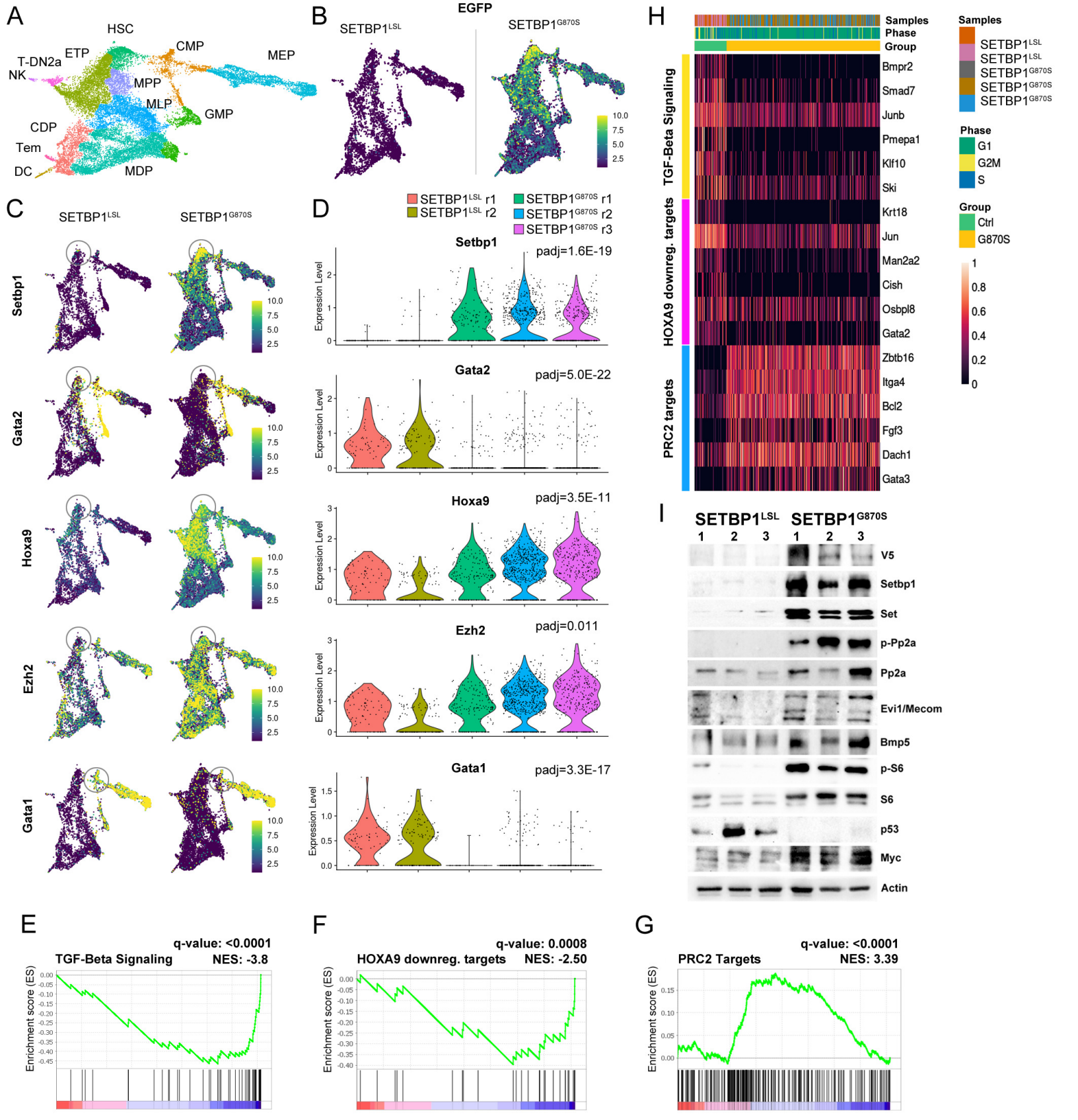
A
HSC
ETP
CMP
MEP
T-DN2a
NK
MPP
MLP
GMP
CDP
Tem
DC
MDP
B
EGFP
SETBP1LSL
SETBP1G870S
10.0
7.5
5.0
2.5
C
SETBP1LSL
SETBP1G870S
Setbp1
Gata2
Hoxa9
Ezh2
Gata1
D
SETBP1LSL r1
SETBP1LSL r2
SETBP1G870S r1
SETBP1G870S r2
SETBP1G870S r3
Setbp1
padj=1.6E-19
Gata2
padj=5.0E-22
Hoxa9
padj=3.5E-11
Ezh2
padj=0.011
Gata1
padj=3.3E-17
Expression Level
H
Samples
Phase
Group
TGF-Beta Signaling
HOXA9 downreg. targets
PRC2 targets
Bmpr2
Smad7
Junb
Pmepa1
Klf10
Ski
Krt18
Jun
Man2a2
Cish
Osbpl8
Gata2
Zbtb16
Itga4
Bcl2
Fgf3
Dach1
Gata3
SETBP1LSL
SETBP1LSL
SETBP1G870S
SETBP1G870S
SETBP1G870S
Phase
G1
G2M
S
Group
Ctrl
G870S
I
SETBP1LSL
SETBP1G870S
1 2 3 1 2 3
V5
Setbp1
Set
p-Pp2a
Pp2a
Evi1/Mecom
Bmp5
p-S6
S6
p53
Myc
Actin
E
q-value: <0.0001
TGF-Beta Signaling
NES: -3.8
Enrichment score (ES)
F
q-value: 0.0008
HOXA9 downreg. targets
NES: -2.50
Enrichment score (ES)
G
q-value: <0.0001
PRC2 Targets
NES: 3.39
Enrichment score (ES)

Figure 4

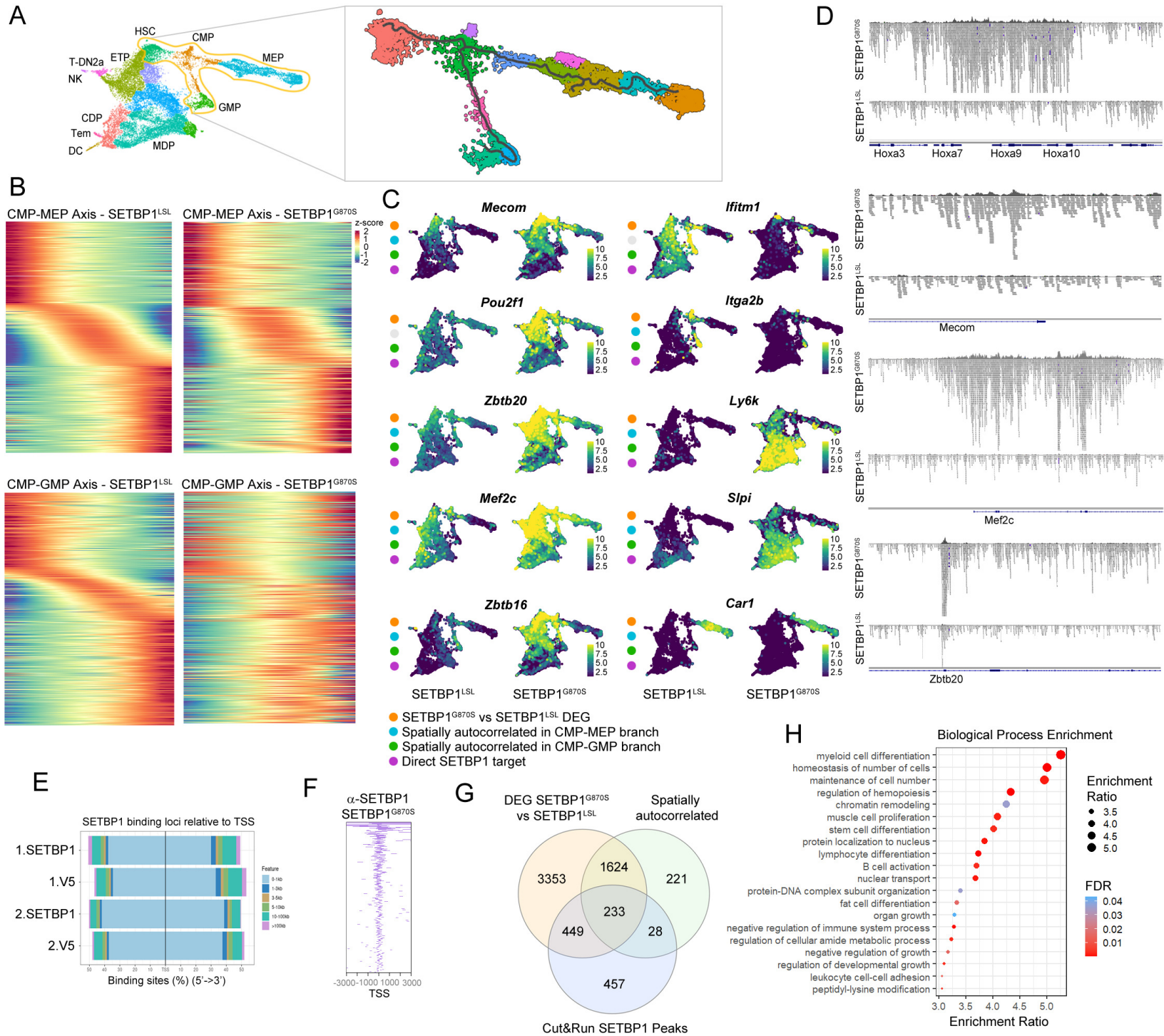
A
HSC
CMP
MEP
T-DN2a
ETP
NK
GMP
CDP
Tem
DC
MDP
B
CMP-MEP Axis - SETBP1LSL
CMP-MEP Axis - SETBP1G870S
z-score
CMP-GMP Axis - SETBP1LSL
CMP-GMP Axis - SETBP1G870S
C
Mecom
Ifitm1
Pou2f1
Itga2b
Zbtb20
Ly6k
Mef2c
Slpi
Zbtb16
Car1
SETBP1LSL
SETBP1G870S
SETBP1G870S vs SETBP1LSL DEG
Spatially autocorrelated in CMP-MEP branch
Spatially autocorrelated in CMP-GMP branch
Direct SETBP1 target
D
SETBP1G870S
SETBP1LSL
Hoxa3
Hoxa7
Hoxa9
Hoxa10
Mecom
Mef2c
Zbtb20
E
SETBP1 binding loci relative to TSS
1.SETBP1
1.V5
2.SETBP1
2.V5
Feature
Binding sites (%) (5'->3')
F
α-SETBP1
SETBP1G870S
-3000-1000 1000 3000
TSS
G
DEG SETBP1G870S vs SETBP1LSL
Spatially autocorrelated
3353
1624
221
233
449
28
457
Cut&Run SETBP1 Peaks
H
Biological Process Enrichment
myeloid cell differentiation
homeostasis of number of cells
maintenance of cell number
regulation of hemopoiesis
chromatin remodeling
muscle cell proliferation
stem cell differentiation
protein localization to nucleus
lymphocyte differentiation
B cell activation
nuclear transport
protein-DNA complex subunit organization
fat cell differentiation
organ growth
negative regulation of immune system process
regulation of cellular amide metabolic process
negative regulation of growth
regulation of developmental growth
leukocyte cell-cell adhesion
peptidyl-lysine modification
Enrichment Ratio
FDR
Enrichment Ratio

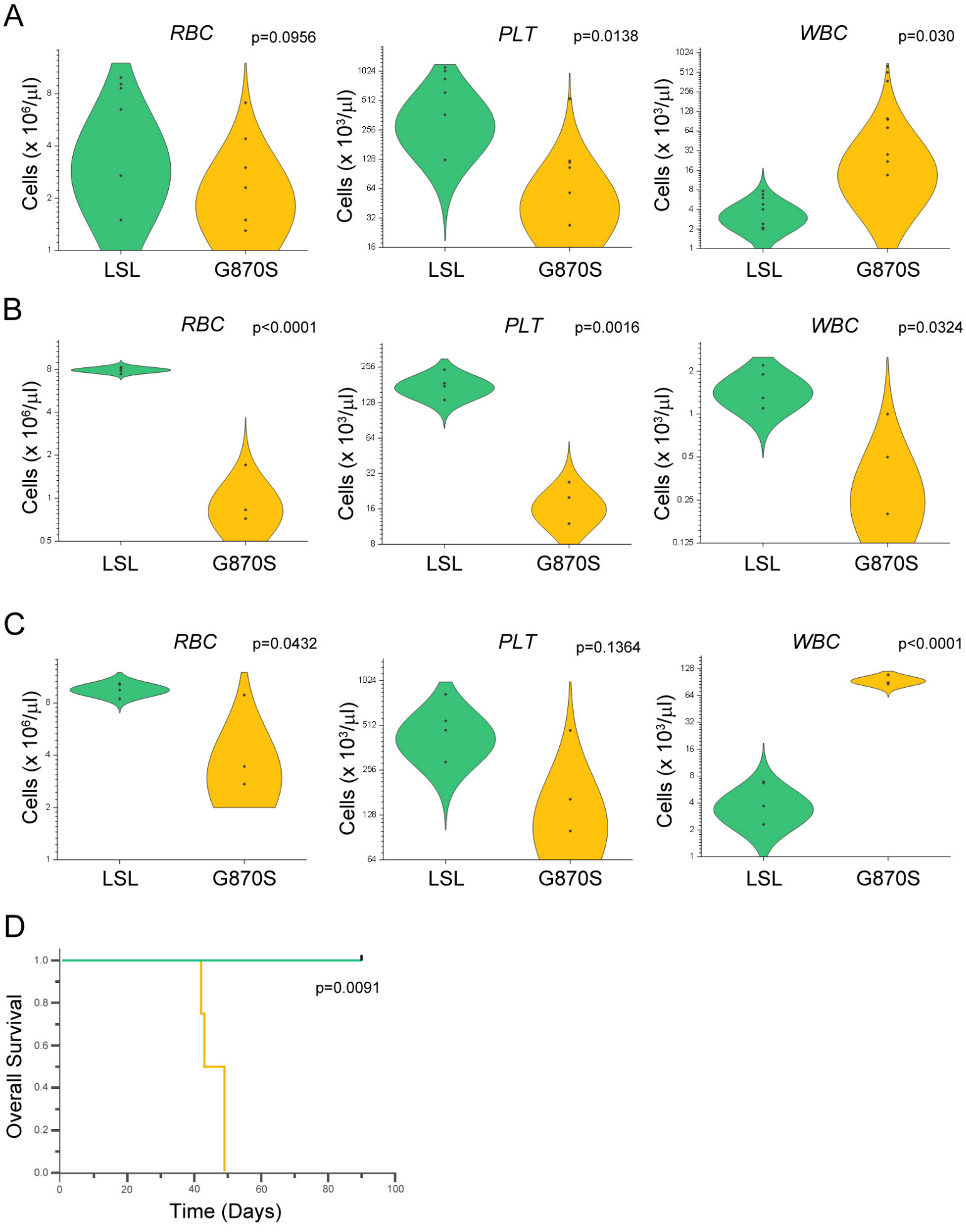
A
RBC
p=0.0956
PLT
p=0.0138
WBC
p=0.030
Cells (x 10⁶/µl)
Cells (x 10³/µl)
LSL
G870S
B
RBC
p<0.0001
PLT
p=0.0016
WBC
p=0.0324
C
RBC
p=0.0432
PLT
p=0.1364
WBC
p<0.0001
D
Overall Survival
Time (Days)
p=0.0091

Figure 6

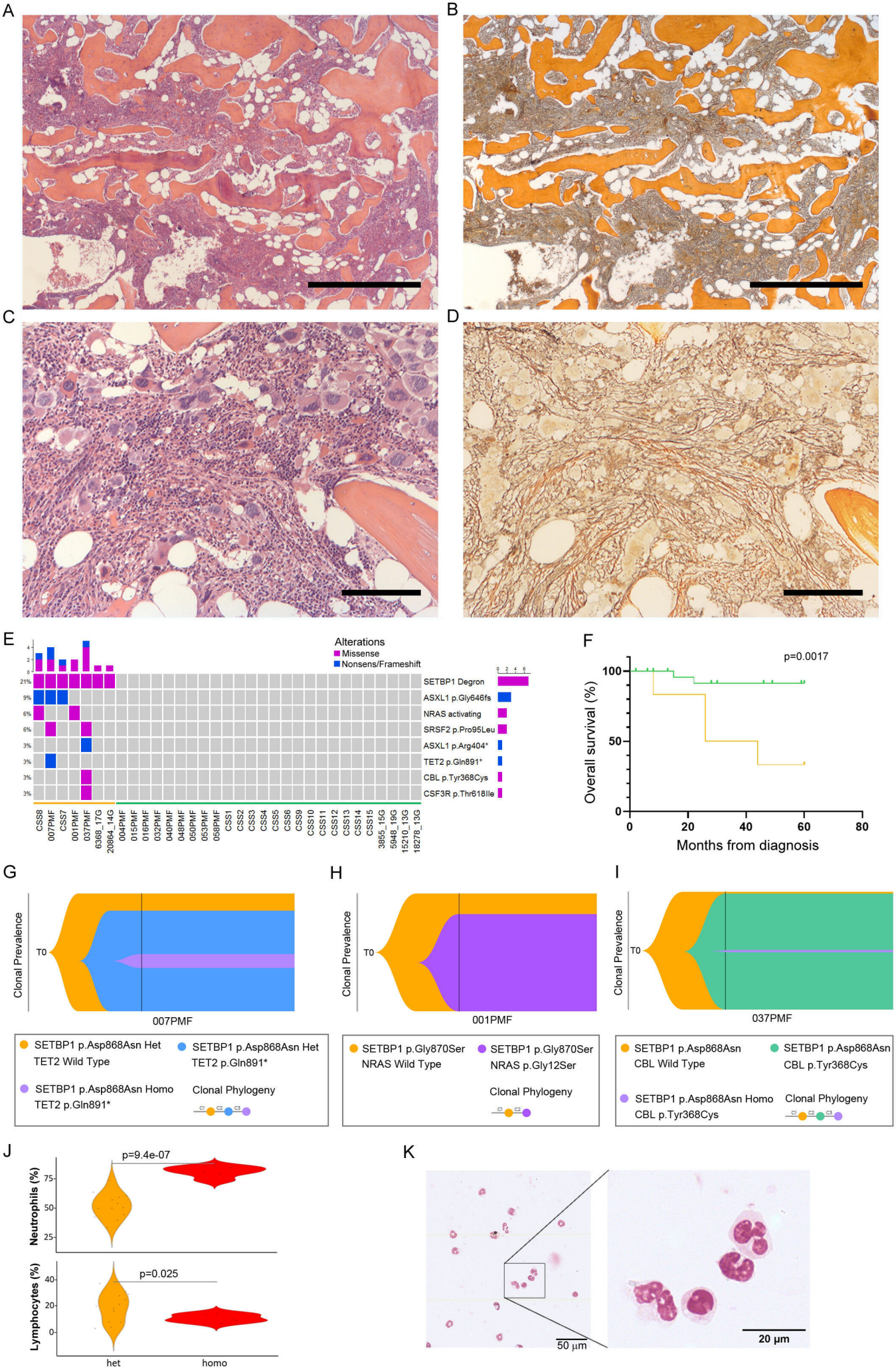
A
B
C
D
E
Alterations
Missense
Nonsens/Frameshift
SETBP1 Degron
ASXL1 p.Gly646fs
NRAS activating
SRSF2 p.Pro95Leu
ASXL1 p.Arg404*
TET2 p.Gln891*
CBL p.Tyr368Cys
CSF3R p.Thr618Ile
21%
9%
6%
6%
3%
3%
3%
3%
CSS8
007PMF
CSS7
001PMF
037PMF
6368_17G
20864_14G
004PMF
015PMF
016PMF
032PMF
040PMF
048PMF
050PMF
053PMF
058PMF
CSS1
CSS2
CSS3
CSS4
CSS5
CSS6
CSS9
CSS10
CSS11
CSS12
CSS13
CSS14
CSS15
3855_15G
5948_19G
15210_13G
18278_13G
F
p=0.0017
Overall survival (%)
100
50
0
0
20
40
60
80
Months from diagnosis
G
Clonal Prevalence
T0
007PMF
SETBP1 p.Asp868Asn Het
TET2 Wild Type
SETBP1 p.Asp868Asn Het
TET2 p.Gln891*
SETBP1 p.Asp868Asn Homo
TET2 p.Gln891*
Clonal Phylogeny
C1
C2
C3
H
Clonal Prevalence
T0
001PMF
SETBP1 p.Gly870Ser
NRAS Wild Type
SETBP1 p.Gly870Ser
NRAS p.Gly12Ser
Clonal Phylogeny
C1
C2
I
Clonal Prevalence
T0
037PMF
SETBP1 p.Asp868Asn
CBL Wild Type
SETBP1 p.Asp868Asn
CBL p.Tyr368Cys
SETBP1 p.Asp868Asn Homo
CBL p.Tyr368Cys
Clonal Phylogeny
C1
C2
C3
J
p=9.4e-07
Neutrophils (%)
75
50
25
p=0.025
Lymphocytes (%)
40
20
0
het
homo
K
50 µm
20 µm

The Role of Somatic *SETBP1* Mutation in the Pathogenesis of an Aggressive Myelofibrosis-Like Myeloproliferative Disorder

Conditional mouse model to investigate the role of *SETBP1* mutation in myeloid malignancy initiation

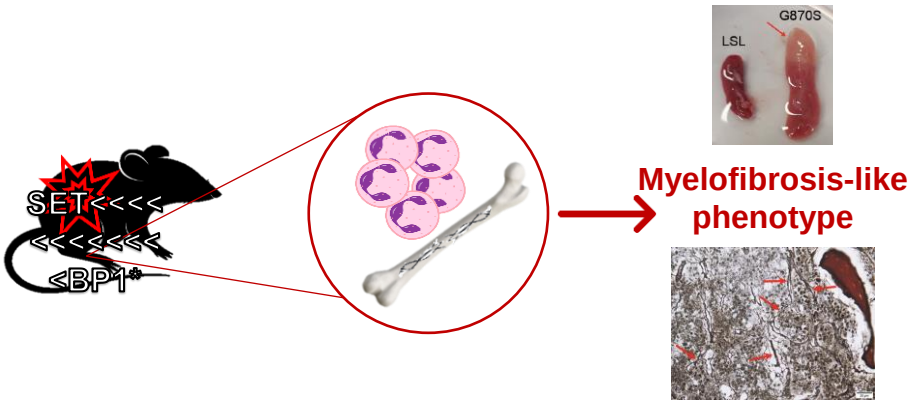

Triple-negative primary myelofibrosis (TN-PMF)

A cohort of 36 patients with PMF that tested negative for somatic mutations in *JAK2*, *MPL*, and *CALR* by high-depth targeted NGS panel (threshold: 1% VAF)

Overall, 14/36 patients fulfilled the criteria of overt PMF and 22 of prefibrotic (early) PMF, according to the WHO 2016 classification

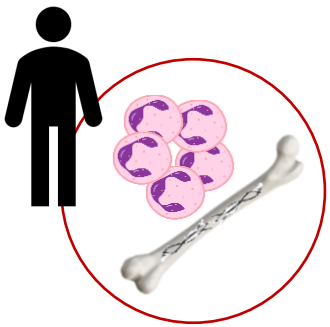

Somatic *SETBP1* mutations identified in 7/36 (19.4%) patients

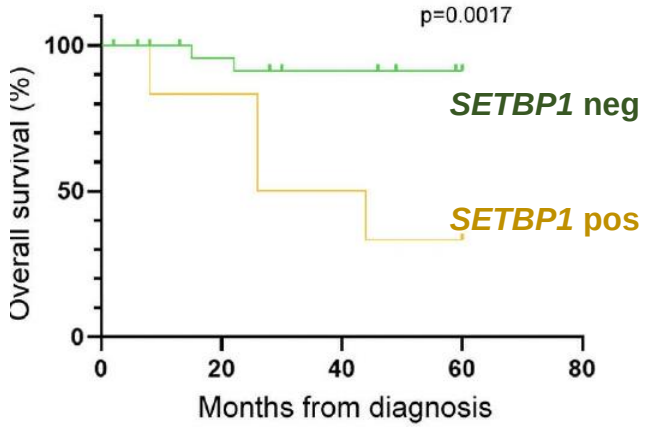

Conclusions: *SETBP1* mutations, acting as a first-hit/early event, drive an aggressive myelofibrosis-like myeloproliferative disorder. Somatic *SETBP1* mutations discriminate between two subtypes of human TN-PMF.

*Crespiatico et al. DOI: 10.xxxx/**blood**.2023xxxxxx*

***Blood* Visual Abstract**